Published OnlineFirst July 12, 2020; DOI: 10.1158/1940-6207.CAPR-19-0538

Multi-omics Analysis Reveals Adipose–tumor Crosstalk in Patients with Colorectal Cancer

Andreana N. Holowatyj[1,2,3,4], Mariam Haffa[5,6], Tengda Lin[1,2], Dominique Scherer[7], Biljana Gigic[7], Jennifer Ose[1,2], Christy A. Warby[1,2], Caroline Himbert[1,2], Clare Abbenhardt-Martin[5,6], David Achaintre[8], Juergen Boehm[1,2], Kenneth M. Boucher[1], Audrey Gicquiau[8], Andrea Gsur[9], Nina Habermann[10], Esther Herpel[6,11], Hans-Ulrich Kauczor[7], Pekka Keski-Rahkonen[8], Matthias Kloor[10], Magnus von Knebel-Doeberitz[10], Dieuwertje E. Kok[12], Johanna Nattenmüller[7], Peter Schirmacher[6,10], Martin Schneider[7], Petra Schrotz-King[5,6], Thomas Simon[13], Per M. Ueland[14], Richard Viskochil[1,2], Matty P. Weijenberg[15], Augustin Scalbert[8], Alexis Ulrich[7], Laura W. Bowers[16,17,18], Stephen D. Hursting[17,18], and Cornelia M. Ulrich[1,2]

ABSTRACT

Obesity and obesity-driven cancer rates are continuing to rise worldwide. We hypothesize that adipocyte–colonocyte interactions are a key driver of obesity-associated cancers. To understand the clinical relevance of visceral adipose tissue in advancing tumor growth, we analyzed paired tumor-adjacent visceral adipose, normal mucosa, and colorectal tumor tissues as well as presurgery blood samples from patients with sporadic colorectal cancer. We report that high peroxisome proliferator-activated receptor gamma (*PPARG*) visceral adipose tissue expression is associated with glycoprotein VI (GPVI) signaling—the major signaling receptor for collagen—as well as fibrosis and adipogenesis pathway signaling in colorectal tumors. These associations were supported by correlations between *PPARG* visceral adipose tissue expression and circulating levels of plasma 4-hydroxyproline and serum intercellular adhesion molecule 1 (ICAM1), as well as gene set enrichment analysis and joint gene-metabolite pathway results integration that yielded significant enrichment of genes defining epithelial-to-mesenchymal transition—as in fibrosis and metastasis—and genes involved in glycolytic metabolism, confirmed this association. We also reveal that elevated prostaglandin-endoperoxide synthase 2 (*PTGS2*) colorectal tumor expression is associated with a fibrotic signature in adipose–tumor crosstalk via GPVI signaling and dendritic cell maturation in visceral adipose tissue. Systemic metabolite and biomarker profiling confirmed that high *PTGS2* expression in colorectal tumors is significantly associated with higher concentrations of serum amyloid A and glycine, and lower concentrations of sphingomyelin, in patients with colorectal cancer. This multi-omics study suggests that adipose–tumor crosstalk in patients with colorectal cancer is a critical microenvironment interaction that could be therapeutically targeted.

See related spotlight by Colacino et al., p. 803

[1]Huntsman Cancer Institute, Salt Lake City, Utah. [2]University of Utah, Salt Lake City, Utah. [3]Vanderbilt University Medical Center, Nashville, Tennessee. [4]Vanderbilt-Ingram Cancer Center, Nashville, Tennessee. [5]German Cancer Research Center (DKFZ), Heidelberg, Germany. [6]National Center for Tumor Diseases (NCT), Heidelberg, Germany. [7]University of Heidelberg, Heidelberg, Germany. [8]International Agency for Research on Cancer (IARC), Lyon, France. [9]Institute of Cancer Research, Medical University of Vienna, Vienna, Austria. [10]European Molecular Biology Laboratory (EMBL), Heidelberg, Germany. [11]University Hospital, Heidelberg, Germany. [12]Wageningen University and Research, Wageningen, The Netherlands. [13]GRN-Clinic, Weinheim, Germany. [14]Maastricht University, Maastricht, the Netherlands. [15]BEVITAL, Bergen, Norway. [16]Purdue University, West Lafayette, Indiana. [17]University of North Carolina, Chapel Hill, North Carolina. [18]Lineberger Comprehensive Cancer Center, Chapel Hill, North Carolina.

Note: Supplementary data for this article are available at Cancer Prevention Research Online (http://cancerprevres.aacrjournals.org/).

Corresponding Authors: Andreana N. Holowatyj, Vanderbilt University Medical Center, Vanderbilt-Ingram Cancer Center, 2525 West End Ave, Suite 334G, Nashville, Tennessee 37203. Phone: 615-322-0105; E-mail: andreana.holowatyj@vumc.org; and Cornelia M. Ulrich, Huntsman Cancer Institute, University of Utah, 2000 Circle of Hope, Room 4725, Salt Lake City, Utah 84112. Phone: 801-213-5716; E-mail: neli.ulrich@hci.utah.edu

Cancer Prev Res 2020;13:817–28

doi: 10.1158/1940-6207.CAPR-19-0538

Introduction

The pandemic rise of obesity worldwide is alarming, with approximately 70% of adults in the United States considered to be overweight or obese (1)—increasing their risk for developing at least 13 distinct types of cancer, including colorectal cancers (2). Adipose tissue, particularly visceral adipose tissue (VAT), not only functions as an energy storage compartment, but is also a dynamic endocrine organ that actively secretes proteins and metabolites involved in the regulation of energy homeostasis and hormonal and inflammatory pathways (3–7). Several obesity-associated cancers, including those of the breast, colorectum, and other gastrointestinal organs, arise either within or in close proximity to adipose depots (5), suggesting that altered adipose tissue metabolism and function may promote nearby tumorigenesis. Although the colon is surrounded by metabolically active VAT in the tumor microenvironment, the colonic epithelium and VAT are spatially distinct (8, 9). Among patients with colorectal cancer, evidence also suggests that body mass index (BMI) poorly correlates with VAT expression profiles (8). However, the associations

Published OnlineFirst July 12, 2020; DOI: 10.1158/1940-6207.CAPR-19-0538

underlying a potential crosstalk between adipose and epithelial tissues and its relevance to carcinogenesis in the colon and other organs remain unknown.

Growth factors (10–13) and inflammatory (14–16) signaling pathways have been shown to be associated with colorectal cancer development, but *in vivo* models suggest that obesity-associated alterations in systemic components of these pathways only explain a fraction of adipose–tumor tissue interactions (15, 17, 18). Here we show via multiple independent -omic measurements and integrated analyses, for the first time, crosstalk between tumor-adjacent VAT and colorectal tumor tissues in patients with colorectal cancer. These results are substantiated in presurgery blood samples by metabolomics and systemic inflammatory and angiogenesis marker profiling. Findings from this multi-omics study suggest that therapeutic strategies aiming to effectively intervene in obesity-related colorectal carcinogenesis might benefit from targeting molecules at the nexus of adipose–tumor crosstalk.

Materials and Methods

Patient population

This study population includes patients from the international prospective ColoCare Study cohort (Clinicaltrials.gov Identifier: NCT02328677; ref. 19). The ColoCare Study cohort includes men and women ages 18–89 years who were diagnosed with a primary invasive colorectal cancer (American Joint Committee on Cancer clinical stages I–IV) undergoing surgery at clinics and sites internationally. The study was approved by the ethics committee of the medical faculty at the University of Heidelberg (Heidelberg, Germany). All study participants provided written informed consent. Electronic medical charts, including pathologic reports, were reviewed to document other clinical parameters. Forty-seven men and women from the ColoCare Study who were recruited in Heidelberg, Germany, between December 2010 and May 2014 had available paired tumor-adjacent VAT, colorectal tumor, and colorectal mucosa tissue samples, and preoperative blood samples, and were diagnosed with microsatellite stable (sporadic) colorectal cancer (**Table 1**).

Table 1. Baseline clinical and demographic characteristics of the colorectal cancer patient cohort: the ColoCare Study.

	Patient cohort	
Characteristic	***n***	**%**
Total	47	
Sex		
Male	37	78.7
Female	10	21.3
Age at diagnosis		
≤39 years	2	4.3
40–49 years	4	8.5
50–59 years	12	25.5
60–69 years	11	23.4
70–79 years	13	27.7
80+ years	5	10.6
Mean, years (SD)	63.5	(12.3)
Race		
White	47	100
Body mass index		
Normal (18.5–≤25 kg/m^2)	13	27.7
Overweight (25–≤30 kg/m^2)	24	51.1
Obese, class I (30–≤35 kg/m^2)	7	14.9
Obese, class II (35+ kg/m^2)	3	6.4
Mean, kg/m^2 (SD)	27.4	(3.8)
Smoking status		
Never smoker	19	40.4
Former smoker[a]	22	46.8
Current smoker	5	10.6
Unknown	1	2.1
NSAID use[b]		
None	31	66.0
Yes	13	27.7
Unknown	3	6.4
Cancer history in first-degree relatives		
None	38	80.9
Yes	7	14.9
Unknown	2	4.3
Microsatellite instability		
Stable (MSS)	47	100
Tumor site		
Colon	21	44.7
Rectum	26	55.3
Tumor grade		
Moderately differentiated	35	74.5
Poorly differentiated	6	12.8
Unknown	6	12.8
Tumor stage		
I	1	2.1
II	18	38.3
III	18	38.3
IV	10	21.3

Abbreviations: NSAIDs, nonsteroidal anti-inflammatory drugs; SD, standard deviation; c, centimeter; kg, kilogram; m, meter.
[a]Former smoker includes individuals who stopped smoking for >2 years.
[b]NSAID use in the last month.

Tissues and blood sample collection

Paired tumor-adjacent VAT ($n = 47$), colorectal tumor ($n = 47$), and normal colorectal mucosa ($n = 47$) tissue samples were prospectively collected during primary tumor resection at the University Hospital Heidelberg (Heidelberg, Germany; ref. 20). Tissue samples were processed by the Tissue Bank of the National Center for Tumor Diseases (NCT, Heidelberg, Germany) in accordance with the regulations of the tissue bank and the approval of the ethics committee the University of Heidelberg (Heidelberg, Germany).

All samples underwent quality control checks to validate VAT sections were without lymph node involvement and tumor viability by a pathologist. Available nonfasting blood samples collected for the ColoCare Study prior to surgery were also available for study inclusion from $n = 47$ patients. Our final analysis cohort consisted of paired tumor-adjacent VAT, colorectal tumor, and colorectal mucosa samples as well as presurgery nonfasting blood samples collected from $n = 47$ patients with sporadic colorectal cancer.

Published OnlineFirst July 12, 2020; DOI: 10.1158/1940-6207.CAPR-19-0538

RNA extraction and transcriptome sequencing

Paired tumor-adjacent VAT, colorectal tumor, and normal mucosa tissue sample preparation, data preprocessing, and quality control/validation techniques are detailed in Haffa and colleagues and Liesenfeld and colleagues (8, 20). Briefly, whole RNA was isolated from fresh-frozen tissue samples using the AllPrep DNA/RNA Mini Kit (Qiagen), and from fresh frozen VAT and SAT samples using the AllPrep DNA/RNA/miRNA Universal Kit (Qiagen) according to the manufacturer's protocols. Tissues were disrupted and homogenized by high-speed shaking with ceramic beads using the Precellys 24 Tissue Lyser (PeqLab Biotechnology). Genomic DNA was removed by DNA spin columns and flow-through was further processed. Remaining DNA was digested by DNase I and whole RNA was extracted using RNA spin columns. Samples obtained from adipose tissue were treated with proteinase K and chloroform to digest and remove proteins prior to the final step of RNA isolation. RNA concentrations were measured using the Epoch Microplate Spectrophotometer (BioTek). RNA quality was determined via the RNA integrity number (RIN) using the Bioanalyzer 2100 (Agilent Technologies). Samples had RINs between 6.3 and 10, and were stored at −80°C until further processing. Transcriptome profiling was performed using the HumanHT-12 Expression BeadChip with 200 ng RNA according to the manufacturer's protocol (Illumina) at the Genomics and Proteomics Core Facility, DKFZ (Heidelberg, Germany).

Plasma metabolomic profiling

Ethylenediaminetetraacetic acid presurgery blood plasma samples from $n = 47$ ColoCare Study participants were collected and processed within 4 hours, according to a standardized protocol, and stored at −80°C as previously described in Geijsen and colleagues (21) To assess data quality, intrabatch and interbatch variabilities were calculated as coefficients of variation for all metabolites based on results obtained for quality control samples. Metabolites were excluded if coefficients of variation (intrabatch and interbatch) were greater than 20%. In cases where a coefficient of variation was greater than 20% for one of the two calculated values, interbatch variability of the Biocrates quality control samples was examined to evaluate data validity. Concentrations below the calibration curve ranges were replaced by the median between zero and the lower limit of quantification (if not more than 5% of metabolite data were missing). Concentrations above the calibration curve were replaced by upper limits of quantification. For compounds semiquantified [Flow Injection Analysis MS-MS (FIA/MS-MS); with one-point calibration), the limit for reporting concentration values was the limit of detection, set to three times the median intensity value of the three PBS zero samples. Given that some compounds measured by FIA with concentration values close to the limit of detection were often detected in a small fraction of the samples, a detection cutoff of less than 10% in $n = 47$ patient samples was used as exclusionary criteria. After quality control, a total of $n = 127$ metabolites were finally retained for subsequent analyses.

Systemic inflammatory and angiogenesis biomarker multiplexing in patient serum

Serum-based assays for multiplexed C-reactive protein, serum amyloid A (*SAA*: measuring *SAA1, SAA2, SAA3*, and *SAA4*), *IL6*, IL8/CXC-motif chemokine 8 (*IL8/CXCL8*), soluble intercellular adhesion molecule 1/cluster of differentiation 54 (*sICAM-1/CD54)*, soluble vascular adhesion molecule 1/cluster of differentiation 106 (*sVCAM-1/CD106*), monocyte chemoattractant protein-1 (*MCP1/CCL2*), VEGF A (*VEGFA*), VEGF D (*VEGFD*), CXC-motif chemokine 12/stromal cell–derived factor 1a (*CXCL12/SDF1a*), and tumor-necrosis factor-a (TNFA) have previously been established on the Mesoscale Discovery Platform (MSD) in Himbert and colleagues (22) Given that selected inflammatory markers generally demonstrated a right skewed distribution, $\log_2$-transformation was applied before model fitting.

Tissue transcriptomic, plasma metabolomic, and serum inflammatory and angiogenesis biomarker analyses

To discern expression changes unique to the colorectal tumor from the mucosal tissue, differences in normalized expression were calculated for each transcript as: Expression = (Normalized tumor expression)–(Normalized mucosa expression). We used this parameter for all subsequent analyses (further referred to as tumor expression). A step-by-step description of our analysis pipeline is outlined in Supplementary Fig. S1.

First, patients were classified as having high ($n = 23$) or low ($n = 24$) expression of *PTGS2* based on the mean expression in tumor tissue. Next, these patient groups were used to calculate the differential expression of VAT transcripts and systemic biomarker levels using Wald tests. Regression model coefficients (β) and *P*-values were estimated for: (i) 47,107 VAT transcripts, (ii) 127 metabolites, and (iii) 11 systemic biomarkers of inflammation and angiogenesis, after adjustment for: patient age at surgery, sex, tumor site (colon/rectum), and stage (I, II, III, IV). Because of the exploratory nature of this research, *P*-values were not FDR-adjusted. $\beta_{Tumor}>0$ indicates that increased expression of a VAT transcript (plasma metabolite or systemic biomarker) is associated with high tumor expression of *PTGS2*. $\beta_{Tumor}<0$ indicates that decreased expression of a VAT transcript (plasma metabolite or systemic biomarker) is associated with low expression of *PTGS2* in the tumor, given other adjustment factors were fixed.

In parallel, patients were classified as having high ($n = 23$) or low ($n = 24$) VAT expression of peroxisome proliferator-activated receptor gamma (*PPARG*) based on the mean expression in VAT. These patient groups were used to calculate the differential expression of tumor transcripts, plasma metabolites, and serum systemic biomarker levels using Wald tests. Regression model coefficients (β) and *P*-values were estimated for: (i) 47,107 tumor transcripts, (ii) 127 metabolites, and (iii) 11 systemic biomarkers of inflammation and angiogenesis, after adjustment for: patient age at surgery, sex, tumor site,

Published OnlineFirst July 12, 2020; DOI: 10.1158/1940-6207.CAPR-19-0538

and stage. Because of the exploratory nature of this research, *P*-values were not FDR-adjusted. $\beta_{VAT}>0$ indicates that increased expression of a tumor transcript (plasma metabolite or systemic biomarker) is associated with high VAT expression of *PPARG*. $\beta_{VAT}<0$ indicates that decreased expression of a tumor transcript (plasma metabolite or systemic biomarker) is associated with low expression of *PPARG* in VAT, given other adjustment factors were fixed.

Ingenuity pathway analysis

Transcripts with fold change [$(2^{\beta})\geq1.2$ or $(2^{\beta})\leq0.8$] and $\alpha<0.05$ were considered to be significant for further investigation. Significant transcripts were entered into Ingenuity pathway analysis (IPA) software (Ingenuity Systems). IPA was used to map transcripts to unique genes, remove duplicate genes, and to classify enriched functions, networks and regulators, diseases, and molecular pathways.

MetaboAnalyst gene-metabolite pathway characterization

To characterize the system-level effects of metabolic and transcriptomic profiles associated with adipose–tumor tissue crosstalk, we integrated multiple -omics results into MetaboAnalyst software (http://www.metaboanalyst.ca/) for enrichment analysis via a joint gene-metabolite pathway mode as previously described in Holowatyj and colleagues (23). In parallel, we imported significant genes ($n = 249$ genes) and metabolites ($n = 4$ metabolites) from *PPARG* analyses for joint gene-metabolite pathway characterization. *Homo sapiens* was selected as the model organism. An overrepresentation analysis, to test if a particular group of compounds is represented more than expected by chance within the compound set, was implemented on the basis of hypergeometric testing to examine whether a particular gene-metabolite set was represented more than expected by chance within the gene and metabolite sets.

Gene set enrichment analysis

Gene set enrichment analysis (GSEA; http://software.broadinstitute.org/gsea/index.jsp) was performed to compute overlaps between $n = 17$ significant genes intersected from *PTGS2* and *PPARG* transcriptomic sequencing analyses and the Hallmark gene sets ($n = 50$; ref. 24). A FDR q-value <0.05 was used as a significance threshold to identify the biologically relevant gene sets. This process resulted in a list of gene sets significantly enriched in molecular signals at the nexus of adipose–tumor crosstalk.

Statistical analysis

The Spearman rank test was used to assess the correlation between continuous variables. Hypothesis testing was done using two-sided tests at a 95% significance level. All analyses were conducted in R statistical software (version 3.1.2) or SAS version 9.4 statistical software (SAS Institute). Graphs were generated from MetaboAnalyst or using Graphpad Prism 7 software.

Results

Given the rising rates of obesity and the challenges for many people to lose excess adipose tissue, an integrated approach to characterizing the crosstalk between adipose and tumor tissues in humans is needed to develop effective mechanism-based strategies for the prevention and control of obesity-driven colorectal cancers. We obtained paired tumor-adjacent VAT, colorectal tumor, and colorectal mucosa tissues as well as preoperative blood samples from patients with primary invasive, microsatellite stable (sporadic) colorectal cancer enrolled in the ColoCare Study ($n = 47$ patients). Tissue samples were collected during surgery to assess for global gene expression, and presurgery blood was collected from individuals to evaluate plasma metabolic profiles ($n = 46$) and serum-based levels of inflammatory and angiogenesis biomarkers ($n = 43$). Transcriptomic profiling using paired colorectal tumor, tumor-adjacent VAT, and colorectal mucosa RNA microarrays was performed on 141 tissue samples ($n = 47$ patients). Fifty-five percent of cases ($n = 26$) were diagnosed with cancers of the rectum/rectosigmoid junction, and BMI of this patient population was classified as overweight (27.4 kg/m^2; **Table 1**). Additional baseline clinical, demographic, and colorectal cancer risk factors of patients are described in **Table 1**.

Role of PPARG VAT expression in adipocyte–colonocyte interactions to promote colorectal carcinogenesis

Obesity-associated proinflammatory cytokines produced in VAT promote adipocyte hypertrophy by inhibiting adipogenesis in part via the suppression of *PPARG*—a master regulator of adipogenesis. As such, we examined tumor-adjacent VAT expression of *PPARG* to evaluate its role in adipocyte–colonocyte interactions that promote colorectal carcinogenesis. First, patients were grouped ($n = 23$ high; $n = 24$ low) by VAT expression of *PPARG* (**Fig. 1**; Supplementary Fig. S1). To examine paracrine effects of crosstalk between VAT and colorectal tumor tissues, plasma-based levels of metabolites and serum-based levels of systemic inflammatory and angiogenesis biomarkers were measured in paired patient presurgery blood samples.

While systemic inflammatory and angiogenesis biomarker profiles did not substantially differentiate *PPARG* VAT expression groups after adjustment for patient age, sex, tumor site, and stage (**Fig. 2A**; Supplementary Table S1)—consistent with previous *in vivo* work (25), we observed that high *PPARG* VAT expression was marginally associated with decreased circulating levels of soluble intercellular adhesion molecule 1 (sICAM1) in humans (FC = 0.81, $P = 0.08$). Moreover, independent interrogation of the paracrine effects of adipose–tumor crosstalk by *PPARG* VAT expression groups via plasma metabolomic profiles revealed 4-hydroxyproline as the top ranked metabolite (FC = 1.53, $P = 0.005$; **Fig. 2B**; Supplementary Table S2). Hydroxyproline is a major component of fibrillar collagen (~13.5% of its amino acid composition), plays a key role in collagen stability, and the quantification of hydroxyproline is utilized to evaluate tissue fibrosis (26)—the

Published OnlineFirst July 12, 2020; DOI: 10.1158/1940-6207.CAPR-19-0538

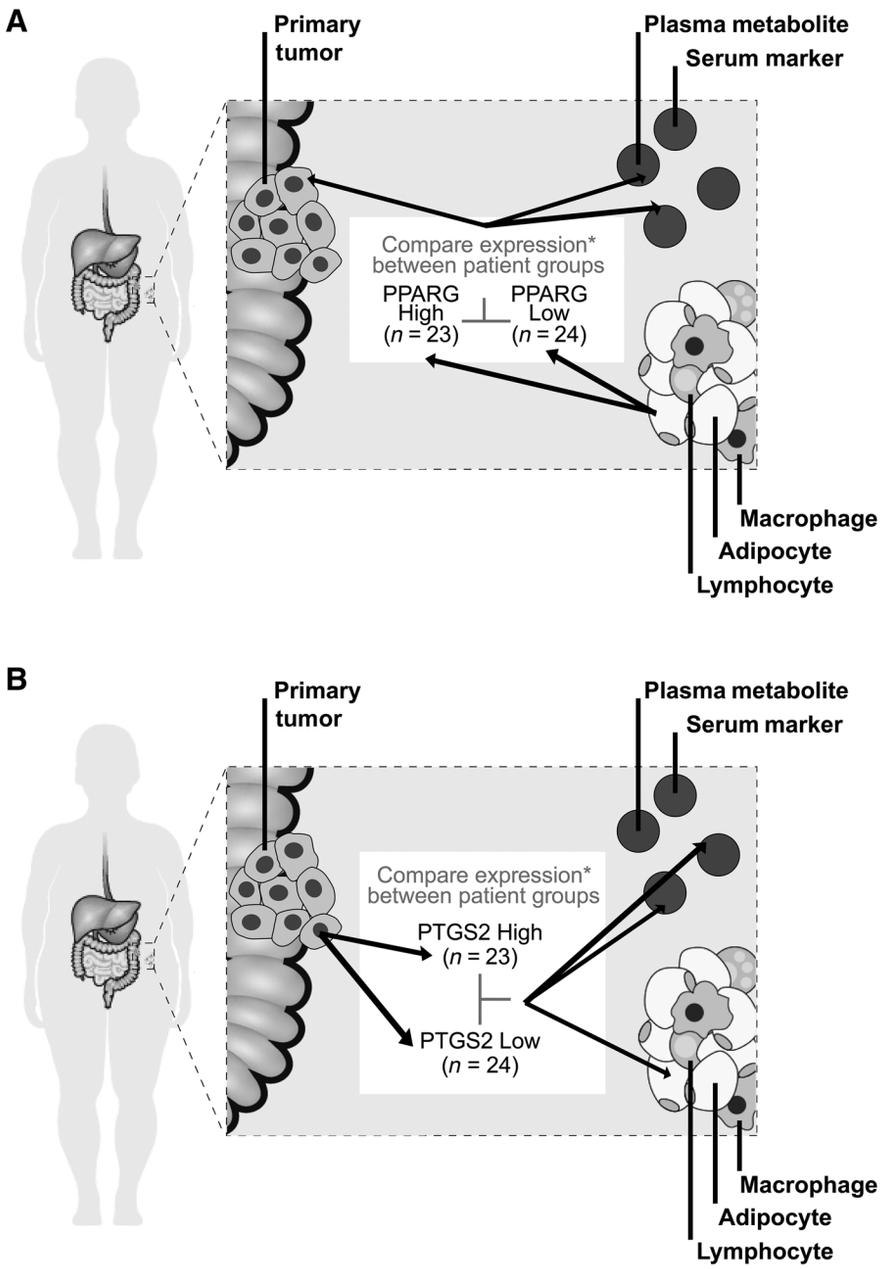

Figure 1.
Schema of tissue transcriptomic, plasma metabolomic, and serum-based biomarker analyses by *PPARG* VAT expression group (**A**) and *PTGS2* colorectal tumor tissue expression group (**B**), for patients with sporadic colorectal cancer. *Regression model coefficients and *P*-values were estimated for tumor transcripts after adjustment for: patient age, sex, tumor site, and stage.

overgrowth of tissues attributed to excess deposition of extracellular matrix components such as collagen. Together with the knowledge that *PPARG* acts as a key regulator of fibrosis, these findings suggest a role for signals associated with fibrosis underlying adipose–tumor crosstalk in patients with colorectal cancer.

Next, transcriptomic analyses of paired colorectal tumor tissue between patients grouped ($n = 23$ high; $n = 24$ low) by VAT expression of *PPARG* was conducted, adjusting for patient age, sex, tumor site, and stage (**Fig. 1**). A total of 249 unique tumor genes were differentially expressed and statistically significant between patient groups (**Fig. 2C**; Supplementary Table S3). Among these tumor genes, over 83% ($n = 207$; 83.1%) were upregulated in association with high *PPARG* VAT expression, including: 11 collagen type molecules (*COL14A1, COL15A1, COL16A1, COL18A1, COL1A2, COL3A1, COL4A1, COL5A2, COL6A1, COL6A2, COL6A3*), dickkopf WNT signaling pathway inhibitor 3 (*DKK3*), frizzled related protein (*FRZB*), hypoxia-inducible factor 1-alpha (*HIF1A*), IGF binding protein 7 (*IGFBP7*), mesenteric estrogen-dependent adipogenesis (*MEDAG*), and WNT1-inducible signaling pathway protein 3 (*WISP3*) genes. These 249 colorectal tumor genes were then curated into IPA software to distinguish enriched molecular pathways. Glycoprotein VI (GPVI) signaling—the

Published OnlineFirst July 12, 2020; DOI: 10.1158/1940-6207.CAPR-19-0538

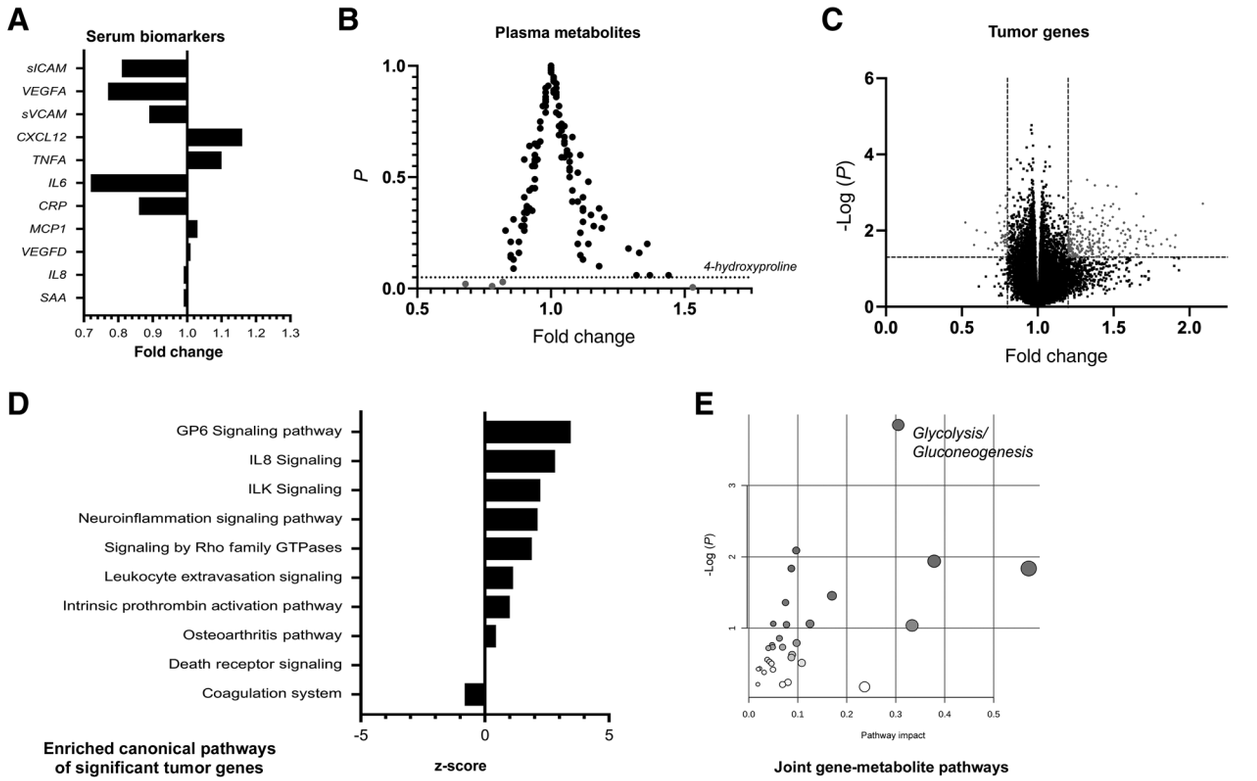

Figure 2.

Elevated *PPARG* VAT expression is associated with tissue fibrosis among patients with sporadic colorectal cancer. Serum-based inflammatory and angiogenesis biomarker levels (**A**) and plasma metabolic concentrations (**B**) associated with differential *PPARG* VAT expression. Differential expression of systemic biomarker levels between high versus low *PPARG* VAT expression patient groups was computed using Wald tests and ranked by fold change. Regression model coefficients and *P*-values were estimated for serum-based biomarkers after adjustment for: patient age, sex, tumor site, and stage. **C,** Volcano plot of gene expression changes in colorectal tumors associated with differential *PPARG* VAT expression. Differential expression of tumor transcripts between high versus low *PPARG* VAT expression groups of patients was computed using Wald tests. Transcripts with absolute value fold change (2^{β})>1.2 and α<0.05 (dashed lines) were considered to be statistically significant. **D,** IPA results of molecular pathways statistically significantly enriched in the $n = 249$ genes differentially expressed in colorectal tumor tissue by *PPARG* VAT expression (high vs. low). **E,** Overrepresentation analysis graphical results of joint gene-metabolite pathways for the significant gene ($n = 249$ colorectal tumor genes from transcriptomic analysis) and metabolite ($n = 4$ metabolites from plasma metabolomics analysis) set. Hypergeometric testing conducted using MetaboAnalyst 4.0 software. Node color shading based on *P*-value and node radius defined by impact values from pathway topology analysis.

major signaling receptor for collagen—emerged as the top ranked canonical pathway (z-score = 3.46, $P = 9.55 \times 10^{-8}$; **Fig. 2D**; Supplementary Table S4). Notably, differentially expressed and statistically significant tumor genes ($n = 249$) were significantly enriched in fibrosis and adipogenesis pathway signaling ($P = 1.58 \times 10^{-13}$; $P = 0.025$; respectively; Supplementary Table S4). *PPARG* ligands and prostaglandins are known to inhibit tyrosine phosphorylation of multiple components of GPVI signaling, indicative of coregulation of several cancer-associated inflammatory pathways identified in our analyses. Together, these findings propose that interacting pathways associated with inflammation, fibrosis, and adipogenesis may be involved in adipose–tumor crosstalk.

To evaluate potential metabolites secreted into plasma by VAT and colorectal tissues, we integrated paired colorectal tumor transcriptomic and plasma metabolomic signatures that distinguish *PPARG* VAT expression groups. Joint gene-metabolite pathway analysis, including these $n = 249$ VAT genes and $n = 4$ plasma metabolites, was conducted via MetaboAnalyst 4.0 software (Supplementary Tables S2 and S3). Glycolysis and gluconeogenesis was the top significantly overrepresented pathway in the colorectal tumor transcriptomic and plasma metabolomic set that distinguishes *PPARG* VAT expression groups (impact score = 0.31, $P = 0.02$; **Fig. 2E**; Supplementary Table S5). Importantly, as *HIF1A* activates *PPARG* and glycolytic genes in response to pathologic stress (27, 28), our transcriptomic findings demonstrate that increased expression of *HIF1A* was also associated with high *PPARG* VAT expression among patients (Supplementary Table S3). As *HIF1A* signaling has been implicated in promoting the fibrotic phenotype of macrophages through the production of profibrotic mediators, including *IL6*, our independent findings from multiple -omic profiles reveal that adipose–tumor crosstalk mediates fibrosis among patients with sporadic colorectal cancer.

Published OnlineFirst July 12, 2020; DOI: 10.1158/1940-6207.CAPR-19-0538

PTGS2/COX2 colorectal tumor expression and a fibrotic signature in adipose–tumor crosstalk

The adipocyte–macrophage paracrine loop promotes and sustains systemic inflammatory changes in association with visceral adiposity, including prostaglandin-endoperoxide synthase 2 (*PTGS2* or *COX2*) upregulation (29). Therefore, it is critical to understand how VAT genes are associated with differential *PTGS2* colorectal tumor expression—a key driver of tumor inflammation. In parallel, patients were grouped ($n =$ 23 high; $n = 24$ low) by *PTGS2* tumor expression (**Fig. 1**; Supplementary Fig. S1). Independent, adjusted comparisons of plasma metabolic profiles ($n = 127$ metabolites; Supplementary Table S6) by *PTGS2* tumor expression groups revealed that $n = 2$ metabolites had significantly different plasma concentrations between patients with high versus low expression of tumor *PTGS2*. Significantly higher concentrations of glycine and lower concentrations of sphingomyelin in patients with sporadic colorectal cancer were observed in patients with high *PTGS2* tumor expression (FC = 1.23, $P = 0.02$; FC = 0.85, $P = 0.047$, respectively; **Fig. 3A**; Supplementary Table S6). Furthermore, independent investigation of systemic inflammatory and angiogenesis biomarker profiles between patients grouped ($n = 23$ high; $n = 24$ low) by *PTGS2* tumor expression revealed that individuals with high expression of *PTGS2* in colorectal tumors were significantly more likely to have higher levels of serum-based SAA—an apolipoprotein and adipokine with potential to enhance lipolysis (FC = 2.13, $P = 0.039$)—and higher levels of IL6, although these findings did not reach statistical significance (FC = 2.38, $P = 0.11$; **Fig. 3B**; Supplementary Table S7). As prior studies have reported that inhibition of *PTGS2* sequentially activates sphingomyelinase in human colon carcinoma cells and sphingolipid signaling has been shown to regulate tissue fibrosis (30–32), these results posit a link between *PTGS2* tumor tissue expression and a fibrotic signature in adipose–tumor crosstalk.

Next, independent multivariable adjusted transcriptomic analyses of paired tumor-adjacent VAT between patient groups were conducted (**Fig. 1**). In total, $n = 129$ unique VAT genes were differentially expressed between patients grouped ($n = 23$ high; $n = 24$ low) by *PTGS2* tumor expression and reached statistical significance (**Fig. 3C**; Supplementary Table S8). Of these VAT genes, 91% ($n = 117$) were found to be upregulated in association with high tumor expression of *PTGS2*. Notably, upregulated VAT genes included: *serum amyloid A2 (SAA2), collagen type genes (COL1A1, COL1A2, COL3A1, COL5A1, COL6A1), C-X-C motif chemokine ligand 12 (CXCL12)*, and *PTGS2*. These $n = 129$ VAT genes were also independently curated into IPA software to classify enriched molecular pathways. Mapping of $n = 129$ VAT genes to canonical pathways identified GPVI signaling as one of the top significant, activated pathways (z-score = 2.45, $P = 0.046$; **Fig. 3D**; Supplementary Table S9). Furthermore, dendritic cell maturation was of particular interest, as it was the top upregulated pathway in patients with high *PTGS2* tumor expression (z-score = 3.0, $P <$ 0.0001; **Fig. 3D**; Supplementary Table S9). Transcriptomic results also substantiated serum-based inflammatory biomarker profile findings (**Fig. 3B**), revealing increased expression of *SAA2* and enrichment of IL6 signaling (z-score = 2.0, $P =$ 0.0002) associated with high tumor *PTGS2* expression among patients with sporadic colorectal cancer (Supplementary Tables S8 and S9). As downregulation of *PPARG* signaling has been shown to result in SAA-induced lipolysis (33), dendritic cells are also known to mediate fibrosis (34, 35), and AT can promote systemic inflammation via *IL6* (36), these findings substantiate that fibrotic signaling may be a key regulator of adipose–tumor crosstalk.

Enrichment of signals associated with fibrosis and glycolytic metabolism at the nexus of adipose–tumor crosstalk

Finally, we sought to gain insight into the biological pathways and potential associations through which molecular signals may mediate adipose–tumor tissue crosstalk. Of the 129 altered genes associated with differential *PTGS2* tumor expression and the 249 genes associated with differential *PPARG* expression in VAT that reached statistical significance (Supplementary Tables S3 and S8), 17 genes were commonly upregulated (**Table 2**). The number of overlapping genes identified ($n = 17$) was substantially higher than the expected number by chance ($n = 1.6$), and we sought to investigate central biological processes in which these 17 signals at the nexus of adipose–tumor tissue crosstalk are enriched. We performed GSEA on "hallmark" gene sets ($n = 50$; ref. 24) which yielded six significant gene sets (**Table 2**). Significantly enriched sets included: genes defining epithelial-to-mesenchymal transition, as in fibrosis and metastasis (FDR q-value $= 1.31 \times 10^{-13}$); and genes encoding proteins involved in glycolysis and gluconeogenesis ($q = 0.02$). Together, these integrated findings posit a key role for signals associated with fibrosis and glycolytic metabolism underlying adipose–tumor crosstalk in patients with colorectal cancer.

Discussion

Adipose tissue, as an endocrine organ, maintains a key role in energy homeostasis and secretes growth factors, hormones, and proinflammatory cytokines that promote a favorable niche for the pathogenesis of colorectal cancer (3, 5, 6, 37). Furthermore, the accumulation of VAT and adipocyte hypertrophy can also promote tumor development (7, 15, 29). However, the underlying associations linking obesity and colorectal cancer remain unknown. Here, via multiple independent -omic measurements of paired tumor-adjacent VAT, colorectal tumor tissues, and presurgery blood samples from patients diagnosed with sporadic colorectal cancer, integrative analyses reveal that fibrosis, GPVI signaling, and glycolytic metabolism, are at the nexus of crosstalk between adipocytes and colonocytes within the tumor microenvironment and may promote colorectal tumor growth.

Published OnlineFirst July 12, 2020; DOI: 10.1158/1940-6207.CAPR-19-0538

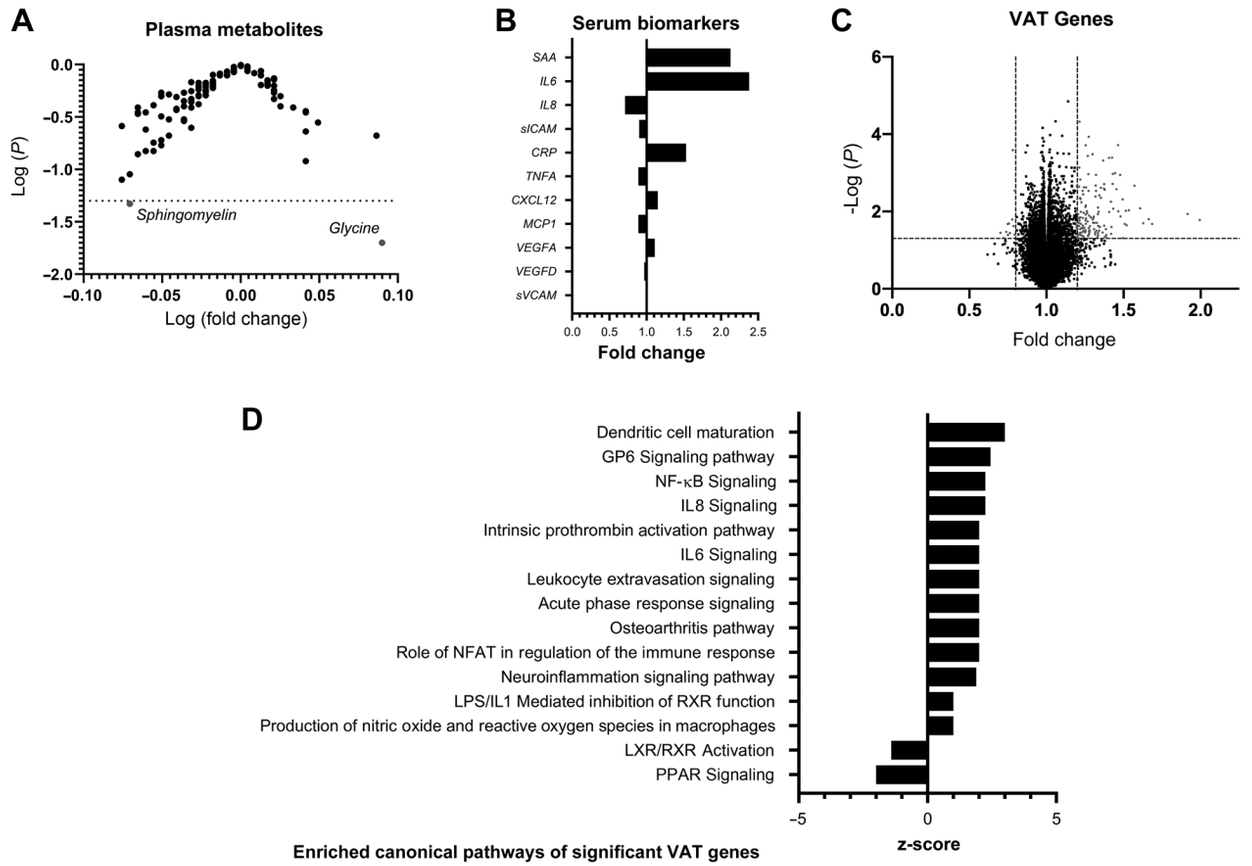

Figure 3.

High *PTGS2* expression in colorectal tumor tissue is linked to a fibrotic signature in adipose–tumor crosstalk among patients with sporadic colorectal cancer. Plasma metabolic concentrations (**A**) and serum-based biomarker levels (**B**) associated with differential *PTGS2* colorectal tumor expression. Differential expression of plasma metabolites and biomarker levels between high versus low *PTGS2* tumor expression patient groups was computed using Wald tests and ranked by fold change. Regression model coefficients and *P*-values were estimated for plasma metabolites and serum-based inflammatory and angiogenesis biomarkers after adjustment for: patient age, sex, tumor site, and stage. Dashed line indicates significance threshold with *P*-value of 0.05. **C,** Volcano plot of VAT gene expression changes associated with differential *PTGS2* tumor expression. Differential expression of VAT transcripts between high versus low *PTGS2* tumor expression patient groups was computed using Wald tests. Transcripts with absolute value fold change >1.2 and α<0.05 (dashed lines) were considered statistically significant. **D,** IPA results of molecular pathways significantly enriched in the $n = 129$ genes differentially expressed in VAT by *PTGS2* tumor expression (high vs. low). Dashed line indicates *P*-value threshold of 0.05.

Abdominal AT accumulation has been associated with metabolic dysfunction and has been shown in animal models (38), in healthy individuals (7), and in patients diagnosed with colorectal cancer (20). *PPARG* is involved in complex systemic physiologic regulatory networks (39, 40). *PPARG* is a nuclear receptor that pairs with retinoid X receptor (RXR) to initiate transcription in multiple tissues, including VAT. After binding to the PPRE DNA binding domain, the PPARG-RXR heterodimer mediated transcription is further regulated by coactivators and corepressors in both a ligand-dependent and independent manner. In the brain, *PPARG* can contribute to weight gain by stimulating food intake as well as increasing adipose tissue mass, along with contributing hepatic insulin sensitivity. In muscle, *PPARG* also influences insulin sensitivity. Previous studies have posited a role for *PPARG* in the obesity-induced colorectal cancer link (41), as *PPARG* has been shown to regulate the expression of molecular mediators involved in the inflammatory response and lipid metabolism (42). Aligned with this evidence, we showed that differential *PPARG* expression in tumor-adjacent VAT is associated with distinct metabolic networks in colorectal tumors, including pathways of glycolytic metabolism. Interestingly, a near-universal component of tumors is the upregulation of glycolysis as an adaptation for hypoxic conditions to promote uncontrolled proliferation and invasion (43, 44). Glycolytic metabolism-related proteins have been associated with tumor maintenance and progression in patients with colorectal cancer (45), and as revealed here, colorectal tumor and VAT genes involved in adipose–tumor crosstalk are enriched in pathways contributing to glycolysis and lipid metabolism.

Preclinical models have also shed light on glycolysis as the major contributor to proinflammatory activation of AT macrophages (46), as AT macrophages from obese mice have been characterized by higher rates of glycolysis and upregulation of

Published OnlineFirst July 12, 2020; DOI: 10.1158/1940-6207.CAPR-19-0538

Table 2. Molecular signals at the nexus of adipose–tumor crosstalk ($n = 17$) are enriched in genes defining epithelial-to-mesenchymal transition, genes encoding proteins involved in glycolysis and gluconeogenesis, and genes regulated by NFκB in response to *TNF* signaling. GSEA results of $n = 17$ significant genes intersected from *PTGS2* and *PPARG* transcriptomic sequencing analyses and the GSEA Hallmark gene sets ($n = 50$). A FDR q-value <0.05 was used as a significance threshold to identify the biologically relevant gene sets.

Pathway			Epithelial-to-mesenchymal transition	Response to ultraviolet radiation	Angiogenesis	Apoptosis	Glycolysis and gluconeogenesis
P			2.63E-15	2.13E-07	2.98E-07	2.77E-05	0.002
FDR *q*-value			1.31E-13	4.97E-06	4.97E-06	3.46E-04	0.021
Gene symbol and name	*COL3A1*	Collagen, type III, alpha 1	■	■	■		
	PDGFRB	Platelet-derived growth factor receptor, beta	■	■		■	
	COL1A2	Collagen, type I, alpha 2	■	■			
	DAB2	Disabled homolog 2, mitogen-responsive phosphoprotein	■	■			
	LUM	Lumican	■		■	■	
	VCAN	Versican	■		■		■
	DCN	Decorin	■			■	■
	SERPINH1	Serpin peptidase inhibitor, clade H, member 1	■				
	PLAU	Plasminogen activator, urokinase					
	EGR2	Early growth response 2					
	COL6A1	Collagen, type VI, alpha 1					
	CYBB	Cytochrome b-245, beta polypeptide					
	MAF	v-maf musculoaponeurotic fibrosarcoma oncogene homolog					
	ARHGDIB	Rho GDP dissociation inhibitor (GDI) beta					
	CPXM1	Carboxypeptidase X, member 1					
	CD248	CD248 molecule, endosialin					
	EMILIN2	Elastin microfibril interfacer 2					

the key metabolic/inflammatory regulator *HIF1A*, compared with lean mice (47). Furthermore, *in vitro* and *in vivo* experiments have shown that NFκB is a critical transcriptional activator of *HIF1A*, as basal NFκB activity is essential for *HIF1A* accumulation under hypoxic conditions (48). In line with this, we also demonstrated among patients with colorectal cancer that high *PPARG* VAT expression is associated with the expression of adhesion molecules in tumors via *HIF1A* and the *TNF* signaling pathway. We detected activation of the *HIF1A-PPARG* axis (28) in our cohort of patients with colorectal cancer, as a significant increase in *HIF1A* tumor expression was associated with high expression of *PPARG* in VAT. In addition, a marginal association between *PPARG* VAT expression and circulating levels of *ICAM1* together with GSEA and joint gene-metabolite pathway findings confirmed this enrichment. Our data also indicate that molecular signals at the nexus of visceral adipose–tumor crosstalk are enriched in genes encoding proteins involved in glycolysis and gluconeogenesis, and genes regulated by NFκB in response to *TNF* signaling. These findings support our hypothesis that adipocyte–colonocyte interactions are a key driver of colorectal cancer. Preclinical studies are warranted to investigate the causal roles of these associations in obesity-induced colorectal cancer progression, and these ongoing studies may lead to novel therapeutic targets to intercept adipocyte–colonocyte crosstalk in colorectal cancer.

Collagens are a highly enriched extracellular matrix component of AT Collagens are a highly enriched extracellular matrix component of AT that provides mechanical support and signaling functions for adipocytes, which are embedded in this matrix (49). Previous *in vitro* work has implicated AT fibrosis as a hallmark of metabolically challenged adipocytes, as hypoxic AT increases profibrotic gene expression and leads to tissue fibrosis (36). In the inflammatory state, the activation of platelets via GPVI signaling has been reported to induce formation of platelet-derived microparticles in the blood—suggesting a key role for GPVI signaling in the amplification of inflammation. Aligned with evidence that platelet microparticles are known to include transcription factors (e.g., *PPARG*) and cytokines and chemokines (e.g., *IL1*), and are hypothesized to function in interactions with other cells (50–53), our multi-omics study reports that key VAT signals from molecular pathways upregulated in patients with high *PTGS2* tumor expression involve interacting pathways associated with fibrosis, including GPVI signaling, dendritic cell maturation, and

Published OnlineFirst July 12, 2020; DOI: 10.1158/1940-6207.CAPR-19-0538

inflammation in patients with colorectal cancer. Our findings were substantiated via independent serum-based inflammatory biomarker profiling, as the elevated expression of *SAA2* and enrichment of IL6 signaling were also associated with high tumor *PTGS2* expression. Together, these results suggest that genes related to GPVI signaling and fibrosis support crosstalk between adipocytes and colonocytes within the tumor microenvironment to drive colorectal tumor growth.

Previous *in vitro* work by Dovizio and colleagues has also suggested that direct cell–cell communication and *PTGS2* overexpression synergistically induced gene expression modifications associated with EMT (51), and that detachment of platelet aggregates from colorectal tumor cells may be a consequence of shedding platelet GPVI receptors. *In vivo* studies have gone on to report specific active targeting of GPVI to fibrotic sites during chronic inflammation, as GPVI binds to collagen fiber and most extracellular matrix proteins. Concordant with these results, here we identified that signals associated with tissue fibrosis, including hydroxyproline, GPVI signaling, sphingolipid signaling, and *PPARG*, underlie adipocyte–colonocyte interactions in patients with colorectal cancer.

We acknowledge the limitations of our study. While our study is the first to discover adipose–tumor crosstalk as a critical interaction between tumors and their surrounding microenvironment in patients with sporadic colorectal cancer, our associations remain descriptive in nature. In addition, our sample size was limited and consisted of predominant rectal cancers, and we were unable to consider other systemic factors—including the influence of the liver on potential *PPARG* crosstalk via circulation. By including only patients with pathologically confirmed microsatellite stable colorectal cancers, we have eliminated genome-wide tumor differences by microsatellite instability status; however, data on colorectal cancer molecular subtypes (e.g., *KRAS/BRAF* mutation status) were not available for this study. We also acknowledge the potential for surgery-associated bias in this study, given the lack of noncancer controls and potential for an acute inflammatory response with surgery-bowel preparation procedures, antibiotics, incisions, and tissue trauma. However, noncancer-related colonic resections are often due to inflammatory causes (e.g., inflammatory bowel disease) that would introduce bias. As all patients underwent surgical resection for colorectal cancer, any impact from surgery would not differ by the factors investigated. Any nondifferential misclassification would attenuate the observed associations between adipocyte–colonocyte interactions within the tumor microenvironment.

Together, our multi-omics findings characterize the molecular phenotype of signals underlying the association between adiposity and colorectal cancer among patients. These results reveal that fibrosis, GPVI signaling, and glycolytic metabolism are at the nexus of crosstalk between adipocytes and colonocytes within the tumor microenvironment and may contribute to colorectal tumor growth. Therapeutic strategies aiming to effectively intervene in obesity-related colorectal carcinogenesis might benefit from targeting molecules at the nexus of the adipose–tumor crosstalk to help reduce the burden of obesity-driven colorectal cancer in patients.

Disclosure of Potential Conflicts of Interest

A.N. Holowatyj reports grants from NIH, Huntsman Cancer Foundation, and University of Utah, Immunology, Inflammation, and Infectious Disease Initiative during the conduct of the study. J. Ose reports grants from NCI during the conduct of the study. C.A. Warby reports grants from NIH (received part of my salary from NIH grants) and other from Huntsman Foundation (received part of my salary from the Huntsman Foundation) during the conduct of the study. H.-U. Kauczor reports grants from Stiftung zur Förderung der Erforschung der Zivilisationserkrankungen during the conduct of the study; Ministerium für Wissenschaft und Kunst Baden-Württemberg outside the submitted work. C.M. Ulrich reports that as center director she formally oversees research funded by a number of companies, including pharmaceutical companies. She has not received any funding for her own research or any funding that could be in conflict with the proposed work. No potential conflicts of interest were disclosed by the other authors.

Authors' Contributions

A.N. Holowatyj: Conceptualization, resources, data curation, formal analysis, supervision, funding acquisition, validation, investigation, visualization, methodology, writing-original draft, project administration, writing-review and editing. **M. Haffa:** Resources, data curation, writing-review and editing. **T. Lin:** Formal analysis, investigation, methodology. **D. Scherer:** Resources, data curation, writing-review and editing. **B. Gigic:** Resources, data curation, writing-review and editing. **J. Ose:** Resources, data curation, writing-review and editing. **C.A. Warby:** Resources, data curation, validation, investigation, writing-review and editing. **C. Himbert:** Data curation, investigation, writing-review and editing. **C. Abbenhardt-Martin:** Resources, data curation, writing-review and editing. **D. Achaintre:** Data curation, investigation, writing-review and editing. **J. Boehm:** Resources, data curation, writing-review and editing. **K.M. Boucher:** Formal analysis, supervision, methodology, writing-review and editing. **A. Gicquiau:** Data curation, formal analysis, writing-review and editing. **A. Gsur:** Data curation, funding acquisition, writing-review and editing. **N. Habermann:** Resources, data curation, funding acquisition, writing-review and editing. **E. Herpel:** Resources, data curation, formal analysis, writing-review and editing. **H.-U. Kauczor:** Resources, data curation, writing-review and editing. **P. Keski-Rahkonen:** Data curation, formal analysis, investigation, writing-review and editing. **M. Kloor:** Resources, data curation, writing-review and editing. **M. von Knebel Doeberitz:** Resources, data curation, writing-review and editing. **D.E. Kok:** Data curation, writing-review and editing. **J. Nattenmüller:** Data curation, writing-review and editing. **P. Schirmacher:** Resources, data curation, writing-review and editing. **M. Schneider:** Resources, data curation, funding acquisition, writing-review and editing. **P. Schrotz-King:** Resources, data curation, writing-review and editing. **T. Simon:** Resources, data curation, writing-review and editing. **P.M. Ueland:** Resources, funding acquisition, writing-review and editing. **R. Viskochil:** Data curation, writing-review and editing. **M.P. Weijenberg:** Resources, funding acquisition, writing-review and editing. **A. Scalbert:** Resources, data curation, formal analysis, supervision, funding acquisition, writing-review and editing. **A. Ulrich:** Resources, data curation, writing-review and editing. **L.W. Bowers:** Conceptualization, investigation, writing-review and editing. **S.D. Hursting:** Conceptualization, resources, formal analysis, supervision, funding acquisition, validation, investigation, visualization, methodology, writing-original draft, project administration, writing-review and editing. **C.M. Ulrich:** Conceptualization, resources, data

Published OnlineFirst July 12, 2020; DOI: 10.1158/1940-6207.CAPR-19-0538

curation, supervision, funding acquisition, investigation, methodology, writing-original draft, project administration, writing-review and editing.

Acknowledgments

A.N. Holowatyj was supported by the NIH under Ruth L. Kirschstein National Research Service Award T32 HG008962 from the National Human Genome Research Institute and by the Vanderbilt University Medical Center. This work was also supported by grants from the NIH/NCI (U01 CA206110, R01 CA189184, R01 CA211705, and R01 CA207371 to C.M. Ulrich; R35 CA197627 to S.D. Hursting), the German Consortium of Translational Cancer Research (DKTK) and the German Cancer Research Center, the Matthias Lackas Foundation, Stiftung LebensBlicke, and Claussen-Simon Stiftung (Germany), the Huntsman Cancer Foundation, and the Immunology, Inflammation, and Infectious Disease Initiative at the University of Utah. This work was also supported by the ERA-NET, JTC 2012 call on Translational Cancer Research (TRANSCAN). The research reported in this publication was supported by the NCI of the NIH under Award Number P30 CA042014. The content is solely the responsibility of the authors and does not necessarily represent the official views of the NIH.

The costs of publication of this article were defrayed in part by the payment of page charges. This article must therefore be hereby marked *advertisement* in accordance with 18 U.S.C. Section 1734 solely to indicate this fact.

Received February 5, 2020; revised May 28, 2020; accepted July 6, 2020; published first July 12, 2020.

References

1. American Cancer Society. Cancer Prevention & Early Detection Facts & Figures 2017–2018. Atlanta: American Cancer Society; 2017.
2. Lauby-Secretan B, Scoccianti C, Loomis D, Grosse Y, Bianchini F, Straif K. Body fatness and cancer–viewpoint of the IARC Working Group. N Engl J Med 2016;375:794–8.
3. Hursting SD, DiGiovanni J, Dannenberg AJ, Azrad M, LeRoith D, Demark-Wahnefried W, et al. Obesity, energy balance, and cancer: new opportunities for prevention. Cancer Prev Res 2012;5:1260–72.
4. Subbaramaiah K, Howe LR, Bhardwaj P, Du B, Gravaghi C, Yantiss RK, et al. Obesity is associated with inflammation and elevated aromatase expression in the mouse mammary gland. Cancer Prev Res 2011;4:329–46.
5. Iyengar NM, Gucalp A, Dannenberg AJ, Hudis CA. Obesity and cancer mechanisms: tumor microenvironment and inflammation. J Clin Oncol 2016;34:4270–6.
6. Zhang Z, Scherer PE. Adipose tissue: the dysfunctional adipocyte - a cancer cell's best friend. Nat Rev Endocrinol 2018;14:132–4.
7. Ulrich CM, Himbert C, Holowatyj AN, Hursting SD. Energy balance and gastrointestinal cancer: risk, interventions, outcomes, and mechanisms. Nat Rev Gastroenterol Hepatol 2018;15:683–98.
8. Haffa M, Holowatyj AN, Kratz M, Toth R, Benner A, Gigic B, et al. Transcriptome profiling of adipose tissue reveals depot-specific metabolic alterations among patients with colorectal cancer. J Clin Endocrinol Metab 2019;104:5225–37.
9. Ose J, Holowatyj AN, Nattenmüller J, Gigic B, Lin T, Himbert C, et al. Metabolomics profiling of visceral and abdominal subcutaneous adipose tissue in colorectal cancer patients: results from the ColoCare study. Cancer Causes Control 2020;31:723–35.
10. Kaaks R, Toniolo P, Akhmedkhanov A, Lukanova A, Biessy C, Dechaud H, et al. Serum C-peptide, insulin-like growth factor (IGF)-I, IGF-binding proteins, and colorectal cancer risk in women. J Natl Cancer Inst 2000;92:1592–600.
11. Ma J, Giovannucci E, Pollak M, Leavitt A, Tao Y, Gaziano JM, et al. A prospective study of plasma C-peptide and colorectal cancer risk in men. J Natl Cancer Inst 2004;96:546–53.
12. Rinaldi S, Cleveland R, Norat T, Biessy C, Rohrmann S, Linseisen J, et al. Serum levels of IGF-I, IGFBP-3 and colorectal cancer risk: results from the EPIC cohort, plus a meta-analysis of prospective studies. Int J Cancer 2010;126:1702–15.
13. Jenab M, Riboli E, Cleveland RJ, Norat T, Rinaldi S, Nieters A, et al. Serum C-peptide, IGFBP-1 and IGFBP-2 and risk of colon and rectal cancers in the European Prospective Investigation into Cancer and Nutrition. Int J Cancer 2007;121:368–76.
14. Mager LF, Wasmer MH, Rau TT, Krebs P. Cytokine-induced modulation of colorectal cancer. Front Oncol 2016;6:96.
15. Yehuda-Shnaidman E, Schwartz B. Mechanisms linking obesity, inflammation and altered metabolism to colon carcinogenesis. Obes Rev 2012;13:1083–95.
16. Toriola AT, Cheng T-YD, Neuhouser ML, Wener MH, Zheng Y, Brown E, et al. Biomarkers of inflammation are associated with colorectal cancer risk in women but are not suitable as early detection markers. Int J Cancer 2013;132:2648–58.
17. Olivo-Marston SE, Hursting SD, Perkins SN, Schetter A, Khan M, Croce C, et al. Effects of calorie restriction and diet-induced obesity on murine colon carcinogenesis, growth and inflammatory factors, and microRNA expression. PLoS One 2014;9:e94765.
18. Zoico E, Rizzatti V, Darra E, Budui SL, Franceschetti G, Vinante F, et al. Morphological and functional changes in the peritumoral adipose tissue of colorectal cancer patients. Obesity (Silver Spring) 2017;25:S87–94.
19. Ulrich CM, Gigic B, Böhm J, Ose J, Viskochil R, Schneider M, et al. The ColoCare Study: a paradigm of transdisciplinary science in colorectal cancer outcomes. Cancer Epidemiol Biomarkers Prev 2019;28:591–601.
20. Liesenfeld DB, Grapov D, Fahrmann JF, Salou M, Scherer D, Toth R, et al. Metabolomics and transcriptomics identify pathway differences between visceral and subcutaneous adipose tissue in colorectal cancer patients: the ColoCare study. Am J Clin Nutr 2015;102:433–43.
21. Geijsen AJMR, Brezina S, Keski-Rahkonen P, Baierl A, Bachleitner-Hofmann T, Bergmann MM, et al. Plasma metabolites associated with colorectal cancer: a discovery-replication strategy. Int J Cancer 2019;145:1221–31.
22. Himbert C, Ose J, Nattenmüller J, Warby CA, Holowatyj AN, Böhm J, et al. Body fatness, adipose tissue compartments, and biomarkers of inflammation and angiogenesis in colorectal cancer: the ColoCare study. Cancer Epidemiol Biomarkers Prev 2019;28:76–82.
23. Holowatyj AN, Gigic B, Herpel E, Scalbert A, Schneider M, Ulrich CM, et al. Distinct molecular phenotype of sporadic colorectal cancers among young patients based on multiomics analysis. Gastroenterology 2020;158:1155–8.e2.
24. Subramanian A, Tamayo P, Mootha VK, Mukherjee S, Ebert BL, Gillette MA, et al. Gene set enrichment analysis: a knowledge-based approach for interpreting genome-wide expression profiles. Proc Natl Acad Sci U S A 2005;102:15545–50.
25. Pasceri V, Wu HD, Willerson JT, Yeh ET. Modulation of vascular inflammation *in vitro* and *in vivo* by peroxisome proliferator-activated receptor-gamma activators. Circulation 2000;101:235–8.
26. Woessner JF Jr. The determination of hydroxyproline in tissue and protein samples containing small proportions of this imino acid. Arch Biochem Biophys 1961;93:440–7.

Published OnlineFirst July 12, 2020; DOI: 10.1158/1940-6207.CAPR-19-0538

27. Narravula S, Colgan SP. Hypoxia-inducible factor 1-mediated inhibition of peroxisome proliferator-activated receptor alpha expression during hypoxia. J Immunol 2001;166:7543–8.
28. Krishnan J, Suter M, Windak R, Krebs T, Felley A, Montessuit C, et al. Activation of a HIF1alpha-PPARgamma axis underlies the integration of glycolytic and lipid anabolic pathways in pathologic cardiac hypertrophy. Cell Metab 2009;9:512–24.
29. Riondino S, Roselli M, Palmirotta R, Della-Morte D, Ferroni P, Guadagni F. Obesity and colorectal cancer: role of adipokines in tumor initiation and progression. World J Gastroenterol 2014;20:5177–90.
30. Sato M, Markiewicz M, Yamanaka M, Bielawska A, Mao C, Obeid LM, et al. Modulation of transforming growth factor-beta (TGF-beta) signaling by endogenous sphingolipid mediators. J Biol Chem 2003;278:9276–82.
31. Martin S, Phillips DC, Szekely-Szucs K, Elghazi L, Desmots F, Houghton JA. Cyclooxygenase-2 inhibition sensitizes human colon carcinoma cells to TRAIL-induced apoptosis through clustering of DR5 and concentrating death-inducing signaling complex components into ceramide-enriched caveolae. Cancer Res 2005;65:11447–58.
32. Shea BS, Tager AM. Sphingolipid regulation of tissue fibrosis. Open Rheumatol J 2012;6:123–9.
33. Liu LR, Lin SP, Chen CC, Chen YJ, Tai CC, Chang SC, et al. Serum amyloid A induces lipolysis by downregulating perilipin through ERK1/2 and PKA signaling pathways. Obesity (Silver Spring) 2011;19:2301–9.
34. Ahadome SD, Mathew R, Reyes NJ, Mettu PS, Cousins SW, Calder VL, et al. Classical dendritic cells mediate fibrosis directly via the retinoic acid pathway in severe eye allergy. JCI Insight 2016;1:e87012.
35. Chen W-Y, Wu S-Y, Lin T-C, Lin S-L, Wu-Hsieh BA. Human dendritic cell-specific ICAM-3-grabbing non-integrin downstream signaling alleviates renal fibrosis via Raf-1 activation in systemic candidiasis. Cell Mol Immunol 2019;16:288–301.
36. Ghaben AL, Scherer PE. Adipogenesis and metabolic health. Nat Rev Mol Cell Biol 2019;20:242–58.
37. Himbert C, Delphan M, Scherer D, Bowers LW, Hursting S, Ulrich CM. Signals from the adipose microenvironment and the obesity-cancer link-a systematic review. Cancer Prev Res 2017;10:494–506.
38. Tran TT, Yamamoto Y, Gesta S, Kahn CR. Beneficial effects of subcutaneous fat transplantation on metabolism. Cell Metab 2008;7:410–20.
39. Rangwala SM, Rhoades B, Shapiro JS, Rich AS, Kim JK, Shulman GI, et al. Genetic modulation of PPARgamma phosphorylation regulates insulin sensitivity. Dev Cell 2003;5:657–63.
40. Hosooka T, Noguchi T, Kotani K, Nakamura T, Sakaue H, Inoue H, et al. Dok1 mediates high-fat diet-induced adipocyte hypertrophy and obesity through modulation of PPAR-gamma phosphorylation. Nat Med 2008;14:188–93.
41. Tontonoz P, Spiegelman BM. Fat and beyond: the diverse biology of PPARgamma. Annu Rev Biochem 2008;77:289–312.
42. Kratz M, Coats BR, Hisert KB, Hagman D, Mutskov V, Peris E, et al. Metabolic dysfunction drives a mechanistically distinct proinflammatory phenotype in adipose tissue macrophages. Cell Metab 2014;20:614–25.
43. Gatenby RA, Gillies RJ. Why do cancers have high aerobic glycolysis? Nat Rev Cancer 2004;4:891–9.
44. Gatenby RA, Gawlinski ET. The glycolytic phenotype in carcinogenesis and tumor invasion: insights through mathematical models. Cancer Res 2003;63:3847–54.
45. Martins SF, Amorim R, Viana-Pereira M, Pinheiro C, Costa RFA, Silva P, et al. Significance of glycolytic metabolism-related protein expression in colorectal cancer, lymph node and hepatic metastasis. BMC Cancer 2016;16:535.
46. Boutens L, Hooiveld GJ, Dhingra S, Cramer RA, Netea MG, Stienstra R. Unique metabolic activation of adipose tissue macrophages in obesity promotes inflammatory responses. Diabetologia 2018;61:942–53.
47. Lumeng CN, Deyoung SM, Bodzin JL, Saltiel AR. Increased inflammatory properties of adipose tissue macrophages recruited during diet-induced obesity. Diabetes 2007;56:16–23.
48. Rius J, Guma M, Schachtrup C, Akassoglou K, Zinkernagel AS, Nizet V, et al. NF-kappaB links innate immunity to the hypoxic response through transcriptional regulation of HIF-1alpha. Nature 2008;453:807–11.
49. Khan T, Muise ES, Iyengar P, Wang ZV, Chandalia M, Abate N, et al. Metabolic dysregulation and adipose tissue fibrosis: role of collagen VI. Mol Cell Biol 2009;29:1575–91.
50. Unsworth AJ, Kriek N, Bye AP, Naran K, Sage T, Flora GD, et al. PPARgamma agonists negatively regulate alphaIIbbeta3 integrin outside-in signaling and platelet function through up-regulation of protein kinase A activity. J Thromb Haemost 2017;15:356–69.
51. Dovizio M, Maier TJ, Alberti S, Di Francesco L, Marcantoni E, Münch G, et al. Pharmacological inhibition of platelet-tumor cell cross-talk prevents platelet-induced overexpression of cyclooxygenase-2 in HT29 human colon carcinoma cells. Mol Pharmacol 2013;84:25–40.
52. Kapur R, Zufferey A, Boilard E, Semple JW. Nouvelle cuisine: platelets served with inflammation. J Immunol 2015;194:5579–87.
53. Beziere N, Fuchs K, Maurer A, Reischl G, Brück J, Ghoreschi K, et al. Imaging fibrosis in inflammatory diseases: targeting the exposed extracellular matrix. Theranostics 2019;9:2868–81.

Published OnlineFirst July 12, 2020; DOI: 10.1158/1940-6207.CAPR-19-0538

Cancer Prevention Research

Multi-omics Analysis Reveals Adipose–tumor Crosstalk in Patients with Colorectal Cancer

Andreana N. Holowatyj, Mariam Haffa, Tengda Lin, et al.

Cancer Prev Res 2020;13:817-828. Published OnlineFirst July 12, 2020.